Development 128, 4881-4890 (2001)
Printed in Great Britain © The Company of Biologists Limited 2001
DEV2779

Essential role of oligodendrocytes in the formation and maintenance of central nervous system nodal regions

Carole Mathis[1], Natalia Denisenko-Nehrbass[2], Jean-Antoine Girault[2] and Emiliana Borrelli[1,*]

[1]Institut de Génétique et de Biologie Moléculaire et Cellulaire, INSERM/CNRS/ULP, BP 163, 67404 Illkirch Cedex, C.U. de Strasbourg, France
[2]INSERM U536, Institut du Fer à Moulin et Collège de France, 75005 Paris, France
*Author for correspondence (e-mail: eb@igbmc.u-strasbg.fr)

Accepted 28 August 2001

SUMMARY

The membrane of myelinated axons is divided into functionally distinct domains characterized by the enrichment of specific proteins. The mechanisms responsible for this organization have not been fully identified. To further address the role of oligodendrocytes in the functional segmentation of the axolemma in vivo, the distribution of nodal (Na^+ channels, ankyrin G), paranodal (paranodin/contactin-associated-protein) and juxtaparanodal (Kv1.1 K^+ channels) axonal markers, was studied in the brain of MBP-TK and *jimpy* mice. In MBP-TK transgenic mice, oligodendrocyte ablation was selectively induced by FIAU treatment before and during the onset of myelination. In *jimpy* mice, oligodendrocytes degenerate spontaneously within the first postnatal weeks after the onset of myelination. Interestingly, in MBP-TK mice treated for 1-20 days with FIAU, despite the ablation of more than 95% of oligodendrocytes, the protein levels of all tested nodal markers was unaltered. Nevertheless, these proteins failed to cluster in the nodal regions. By contrast, in *jimpy* mice, despite a diffused localization of paranodin, the formation of nodal clusters of Na^+ channels and ankyrin G was observed. Furthermore, K^+ channels clusters were transiently visible, but were in direct contact with nodal markers. These results demonstrate that the organization of functional domains in myelinated axons is oligodendrocyte dependent. They also show that the presence of these cells is a requirement for the maintenance of nodal and paranodal regions.

Key words: Oligodendrocyte, MBP-TK, *jimpy*, Mouse, Ranvier's node

INTRODUCTION

Ion fluxes in mammalian myelinated axons are restricted to the nodes of Ranvier, where, in particular, voltage-gated Na^+ channels are clustered at a high density. This organization accelerates nerve impulse propagation with reduced energy and an efficient employment of space. The nodes of Ranvier are separated from the internodes by two distinct domains of the axolemma: the paranodal axoglial junctions and the juxtaparanodal regions (Salzer, 1997). Each of these domains is characterized by the presence of specific protein complexes. Levels of Na^+ channels, ankyrin G and cell adhesion molecules (e.g. NrCAM and 186 kDa neurofascin) are highly enriched at the nodes (Peles and Salzer, 2000). At the level of the paranodes, oligodendrocytes are anchored to axons through septate-like junctions that are characterized by the enrichment of paranodin/contactin-associated-protein (Caspr; Nrxn4 – Mouse Genome Informatics), an axonal glycoprotein associated with contactin (Einheber et al., 1997; Menegoz et al., 1997; Rios et al., 2000). Shaker-type K^+ channels are clustered in the juxtaparanodal regions (Wang et al., 1993) in association with Caspr2 (Poliak et al., 1999). In spite of the recent progress in the identification of the protein complexes that are present along the axonal membrane, the molecular mechanisms leading to their asymmetric distribution are not well understood in the CNS (Rasband and Shrager, 2000; Salzer, 1997; Trapp and Kidd, 2000).

In the rodent CNS, the onset of myelination coincides with the clustering of voltage-dependent Na^+ channels at the developing nodes of Ranvier (Rasband et al., 1999a). In vitro, oligodendrocytes appear to secrete a soluble factor responsible for the formation of Na^+ channels and ankyrin G clusters (Kaplan et al., 1997), indicating that cluster formation may not require a direct axoglial contact. By contrast, in vivo studies suggest that paranodal contacts are required for the clustering of Na^+ and K^+ channels (Rasband et al., 1999b). It has been proposed that paranodal junctions play a central role in the organization of nodal regions (Rasband and Shrager, 2000; Trapp and Kidd, 2000). Interestingly, however, in galactolipid-deficient mice ($Cgt^{-/-}$ mice; $Ugt8^{-/-}$ – Mouse Genome Informatics), which display abnormal paranodal axoglial junctions, paranodin is diffusely distributed along the axon. In these mice, the location of K^+ channels clusters is altered, whereas Na^+ channels are less affected (Dupree et al., 1999).

To analyze the implication of oligodendrocytes in the formation of nodal domains, we used two dysmyelinating

mutant animals, the MBP-TK (Mathis et al., 2000) and the *jimpy* mice (Sidman et al., 1964). In these animals, severe oligodendrocyte alterations occur at different stages during the postnatal period. Ablation of oligodendrocytes in the CNS either before or during the onset of myelination was induced by treating MBP-TK mice with FIAU, a nucleoside analogue (Mathis et al., 2000). In *jimpy* mice, delayed oligodendrocyte damage and death occurs spontaneously during the first postnatal weeks (Knapp et al., 1986; Meier and Bischoff, 1974; Vermeesch et al., 1990). The analysis of these two mutants reveals the essential, but distinct roles of oligodendrocytes in the formation and maintenance of both the nodes of Ranvier and the adjacent paranodal regions.

MATERIALS AND METHODS

Animals

Transgenic mice used in this study were generated as described (Mathis et al., 2000). All transgenic and wild-type control animals were obtained by mating heterozygous MBP-TK females with C57BL6 males. For each experiment, siblings were treated with the nucleoside analog, FIAU (1-(2-deoxy-2-fluoro-β-δ-arabinofuranosyl)-5-iodouracil). Treatments were performed with daily subcutaneous injections of FIAU (40 mg/kg) in phosphate-buffered saline (PBS) as described (Mathis et al., 2000). 1-20d, 1-6d and 6-20d refers to the treatment protocols used. For each of these treatments, animals were killed at 21 days. Genotyping was performed as previously described (Mathis et al., 2000). *jimpy* mutant mice were generated by mating heterozygous females with wild-type males. Mice were sacrificed at 15 (P15) or 21 (P21) days after birth. Wild-type littermates were used as controls.

Immunohistology

Wild-type and MBP-TK-treated animals were killed and their brains were directly embedded in OCT (Tissue-Tek) and frozen in dry ice. Sagittal sections (10 μm) were cut on the cryostat, thaw-mounted onto gelatin-coated slides and stored at –80°C until immunofluorescence experiments were performed. The sections were post-fixed in formalin solution (Sigma) for 15 minutes, or methanol/acetone (50/50 vol/vol at –20°C), for labeling with ankyrin G antibodies, and pre-incubated for 1 hour in 5% normal goat serum (Vector Laboratories), 0.05% Tween 20 in PBS at room temperature, followed by incubation with primary antibodies (at the appropriate dilution) at 4°C overnight. Slides were then incubated for 1 hour with the secondary antibodies. Primary antibody dilutions were: rabbit anti-paranodin SL51 (1:1000-1:4000) (Menegoz et al., 1997), mouse anti-Kv1.1 α-subunit (1:100, Upstate Biotechnology), mouse anti-ankyrin G (1:100-1:500, Zymed Laboratories), mouse anti-Na^+ channel PAN (1:100, Sigma), rabbit anti-Na^+ channel (1:100, a gift from Dr R. Levinson, Colorado University Health Science Center) and mouse anti-MBP (67-74) (1:1500, Chemicon). Goat anti-rabbit IgG conjugated with Alexa Fluor 594, and goat anti-mouse conjugated with Alexa Fluor 488 (Molecular Probes) were used at a dilution of 1:600, and goat anti-rabbit IgG conjugated with FITC (Silenus) was used at a dilution of 1:200. Double-immunolabeling with anti-MBP and anti-paranodin antibodies was performed on brain sections fixed in Bouin solution and embedded in paraffin. Before incubation with the antibodies, paraffin was removed and the brain sections were re-hydrated. Immunolabeled sections were examined with a conventional microscope (Zeiss Axiophot) or with a confocal microscope (DMRE Leica). Controls were always performed by omitting the primary antibodies.

Immunoblot analysis

Brains from chronically treated (1-20d) wild-type and MBP-TK mice were rapidly dissected and put in liquid nitrogen. Tissues were homogenized in 1 ml of lysis buffer (5 mM EDTA, 10 mM Tris pH 7.5, 1% SDS, 5 μg/ml PMSF, 1 mM NaF, 1 mM Na3VO4, 1 μg/ml leupeptin, 1 μg/ml aprotinin). Protein concentrations of the lysates were determined by the Micro BCA method (Pierce Chemical, Rockford, IL). Protein extracts were separated by SDS/PAGE and transferred to nitrocellulose membrane. Each lane was loaded with 10 μg (for paranodin) or 30 μg (for K^+ and Na^+ channels) of protein extracts. Blots were blocked in 3% skim milk in 1× PBS, 0.02% Tween 20, and incubated overnight with primary antibodies. Primary antibodies were used at the following dilutions: rabbit anti-paranodin SL51 1:2000, mouse anti-Kv1.1 α-subunit 1:1000 (Upstate Biotechnology) and mouse anti-Na^+ channel PAN 1:1000 (Sigma). Blots were then incubated with either horseradish peroxidase (HRP)-conjugated goat anti-rabbit IgG (1: 10000) or HRP-conjugated horse anti-mouse IgG (1:10000). Signals were developed in enhanced chemiluminescence (ECL) western blotting detection reagents (Amersham, UK). Quantification of each immunoblot was performed by scanning autoradiographs with an imaging densitometer apparatus (BioRad) and by measuring band intensity using the molecular analyst software (BioRad). The level of protein extracts loaded in each lane was controlled by staining the blots with Ponceau Red (Sigma). The reported results were obtained by the analysis of animals from three different experiments. Protein extracts from both genotypes were always concomitantly analyzed on the same gel.

Quantification of nodal elements

Immunolabeled brain cryosections from wild-type and MBP-TK mice treated with different schedules of FIAU injections (1-20d, 1-6d, 6-20d) were used to count the number of binary or single paranodes (paranodin-positive) as well as the number of ankyrin G, Na^+ and K^+ channel clusters. Quantification was performed in the corpus callosum. Anatomically matched brain sections of wild-type and MBP-TK siblings identically treated were taken for this quantification. The number of random fields of view (FOV=1000 μm^2) examined varies between 50 and 200. Statistical analysis was performed by ANOVA. Values represent mean±s.e.m. Statistical significance was assessed by post-hoc analysis (Fisher's test).

RESULTS

The nodal clustering of axonal proteins disappears in the absence of oligodendrocytes

To trigger specific oligodendrocyte cell death at different stages of development, we used MBP-TK mice. In these mice, the myelin basic protein (MBP) gene promoter drives the expression of a toxigene, the herpes virus thymidine kinase (Borrelli et al., 1988). This transgene is not toxic by itself, unless the transgenic animals are treated with a nucleoside analog, such as FIAU (Borrelli et al., 1988). Using different schedules of FIAU treatment, we have been able to induce various degrees of dysmyelination in the CNS of MBP-TK mice (Mathis et al., 2000). We used this model system to study how the distribution of axonal proteins, normally localized in the node of Ranvier, are affected by the loss of oligodendroglial signals. Immunohistological analyses were performed on brain sections from MBP-TK and wild-type littermates, both chronically treated with FIAU from postnatal day 1 to 20 (1-20d). We have previously shown that this treatment results in a 95% reduction of oligodendrocytes and consequently of MBP expression in MBP-TK mice compared with wild-type siblings (Mathis et al., 2000). In order to analyze nodal organization in myelinated axons, we used four specific antibodies against axonal

proteins that are normally enriched in paranodes (paranodin), juxtaparanodal regions (Kv1.1, *shaker*-type K^+ channels), or nodes of Ranvier (voltage-gated Na^+ channels and ankyrin G).

Normal binary paranodin-positive clusters corresponding to paranodes were observed in the corpus callosum of 21-day-old wild-type mice (Fig. 1A,C,E). Na^+ or ankyrin G immunopositive zones, which define the nodal regions, were identified in contact with paranodin positive clusters (Fig. 1A,B). K^+ channel clusters were also easily identifiable at this age, located on the lateral side of the binary paranodin-positive clusters, and corresponding to the juxtaparanodal regions (Fig. 1E). These results are in agreement with the known location of these proteins (Peles, 2000), and clearly show the absence of any nonspecific effects that could be due to the FIAU treatment in wild-type mice.

In 1-20d FIAU-treated MBP-TK mice, the distribution of all of the nodal markers was dramatically altered. Paranodin immunoreactivity appeared diffuse, instead to be concentrated in specific domains (Fig. 1B,D,F). Furthermore, the localization of ankyrin G- and Na^+ channel-positive clusters was also profoundly altered, with an almost complete disappearance of the nodal clusters and a diffuse staining along the axons (Fig. 1B,D). Only in rare instances were broad, poorly defined and weakly immunoreactive clusters observed. Double immunostaining using antibodies directed against Na^+ channels and ankyrin G, showed a colocalization of these proteins in these broad nodes (Fig. 1D, inset). Quantification of these clusters showed a higher number of these specimens in the 1-20d transgenic treated mice than in wild-type controls (MBP-TK, 1.01±0,15/FOV; wild type, 0.28±0,15/FOV, n=20). These figures might represent an early immature stage of node formation.

Interestingly, the absence of oligodendrocytes in MBP-TK mice resulted in a complete diffusion of Kv1.1 immunostaining (Fig. 1F). Thus, massive death of oligodendrocytes at early stages of postnatal development led to a complete failure in the organization of axonal membrane domains.

Oligodendrocyte ablation does not change the protein levels of paranodin, Na^+ channels and Kv1.1

As the absence of oligodendrocytes had such profound effects on the distribution of nodal and paranodal proteins, we examined whether the levels of expression of these proteins were also altered. Total protein extracts were prepared from the cerebral hemispheres of 1-20d FIAU-treated wild-type and MBP-TK mice. A band of the expected size and equal intensity corresponding to paranodin was detected in extracts from both wild-type and MBP-TK-treated mice (Fig. 2). This result is consistent with previous studies that revealed no difference in the level of paranodin expression in other animal models (Dupree et al., 1999). Similarly, western blot analyses revealed no difference between both genotypes in the levels of K^+ and Na^+ channels (Fig. 2).

An upregulation of K^+ and Na^+ channel expression has been reported in the CNS of adult *shiverer* and *trembler* mice (Noebels et al., 1991; Wang et al., 1995; Westenbroek et al., 1992). A similar upregulation of Na^+ channels has been observed in multiple sclerosis patients at the site of lesions (Moll et al., 1991). The absence of such upregulation in treated MBP-TK mice might be explained by the age of the mice when the experiments were performed (3 weeks). Indeed, the increased expression of ion channels was previously documented in adult animals and might represent a late compensatory mechanism in response to the abnormal electrical activity of dysmyelinated axons. Our data suggest that the level of expression of axonal nodal and paranodal proteins is independent of oligodendrocyte presence and, consequently, of myelination in the first postnatal weeks. Nevertheless, it cannot be excluded the presence of differences in the turnover of these proteins after oligodendrocytes ablation.

The severity of axonal alterations in the nodal region correlates with the degree of dysmyelination in MBP-TK mice

The degree of dysmyelination in MBP-TK mice depends on the timing of FIAU treatment with respect to oligodendrocyte differentiation (Mathis et al., 2000). Three distinct protocols of FIAU administration were used to address more precisely the role of oligodendrocytes in the formation of the nodal regions during development. The 1-20d chronic treatment described above induced a massive disappearance of MBP staining in the cerebral cortex and corpus callosum in MBP-TK mice (Fig. 3, compare A with B). Additional groups of mice were treated from postnatal day 1 to 6 (1-6d) or from postnatal day 6 to 20 (6-20d). All animals were killed at the age of three weeks. We have already shown that these two latter protocols (1-6d and 6-20d) resulted in a 50% reduction of oligodendrocytes and myelin, with a similar decrease in the level of MBP mRNA expression in the whole brain (Mathis et al., 2000). However, the two treatments had different effects on the myelination of the corpus callosum. Immunohistological studies using anti-MBP antibodies revealed a higher number of myelinated fibers in the corpus callosum of the transgenic mice treated from days 6 to 20 (Fig. 3D) when compared with mice treated from days 1 to 6 (Fig. 3C).

We have quantified the number of binary and single paranodes, as well as the number of nodal and juxtaparanodal clusters in the corpus callosum in each group of treated mice. The results were compared with those obtained in wild-type siblings, which had received the same treatment (Table 1). It should be noted that at 21 days, myelination is not complete and many single paranodes were present in wild-type mice.

In MBP-TK mice treated from days 1 to 20 (1-20d), virtually no binary and few single paranodes (5% of wild type) were observed (Table 1). The reduction of nodal clustering of Na^+ channels and ankyrin G was similar and dramatic (8 and 7% of wild type, respectively). In addition, Kv1.1-positive clusters were completely absent in transgenic treated mice (Table 1).

Interestingly, MBP-TK animals treated during the first 6 days after birth (1-6d) presented a much stronger perturbation of nodal, paranodal and juxtaparanodal regions than transgenics treated from day 6 to 20 (Table 1). In 1-6d MBP-TK mice, the number of binary paranodes and single paranodes was strongly reduced (19% and 34% of wild type, respectively). By contrast, a milder reduction of binary and single paranodes was observed in 6-20d transgenic mice (43% and 72% of wild type, respectively). Similarly, the number of preserved Na^+ channels and ankyrin G clusters were different depending on the timing of FIAU treatment (Table 1). They were respectively estimated at 39% and 69% of wild type, in 1-6d mutant mice, whereas they were 56% and 90%, respectively, in 6-20d mutant mice. Finally, the number of

Table 1. Quantification of the oligodendrocyte-dependent variation in the number of the different elements of the node of Ranvier

	MBP-TK			
	1-20d	1-6d	6-20d	Control
Binary paranodes PND$^+$	0.006±0.006**	0.29±0.06**	0.67±0.06**	1.56±0.07
Single paranodes PND$^+$	0.12±0.027**	0.84±0.14**	1.76±0.11**	2.44±0.05
Na$^+$-channel clusters	0.21±0.07**	1.01±0.11**	1.47±0.12**	2.61±0.06
Ankyrin G-positive nodes	0.15±0.09**	1.54±0.14*	1.94±0.13	2.17±0.17
K$^+$-channel clusters	0**	0.08±0.04**	0.27±0.08**	1.22±0.08

Values (mean±s.e.m.) correspond to quantification of the various elements of the node/field of view using axonal compartment-specific antibodies as indicated. Three different schedules of FIAU administration were used, which resulted in various degrees of oligodendrocyte ablation. Values from treated MBP-TK animals were always compared with the control. (ANOVA; Fisher's post-hoc analysis: *P<0.02; **P<0.0001.)

juxtaparanodal K$^+$ channel clusters was highly reduced in both groups with respect to wild type, with only 7% residual clusters in 1-6d and 22% in 6-20d mutant mice.

These results show a correlation between the number of oligodendrocytes able to myelinate and the resulting number of nodes and paranodes. This further supports the requirement of oligodendrocytes for nodal region formation. In addition, this quantitative approach allowed several interesting observations. First, a higher number of single paranodes over binary paranodes was observed in all groups of mice. This is likely to result from the presence of only partially myelinated fibers, with gaps in oligodendrocyte sheaths along their length (see Fig. 3F). Second, the paranodal and juxtaparanodal clusters were proportionally more severely affected than the nodal clusters, in all groups of mutant mice. Finally, in 1-6d and 6-20d mutant mice, the number of Na$^+$ channel clusters was lower than that of ankyrin G clusters. This difference is very likely to be due to the early clustering of ankyrin G compared with Na$^+$ channels in node formation (Rasband et al., 1999a).

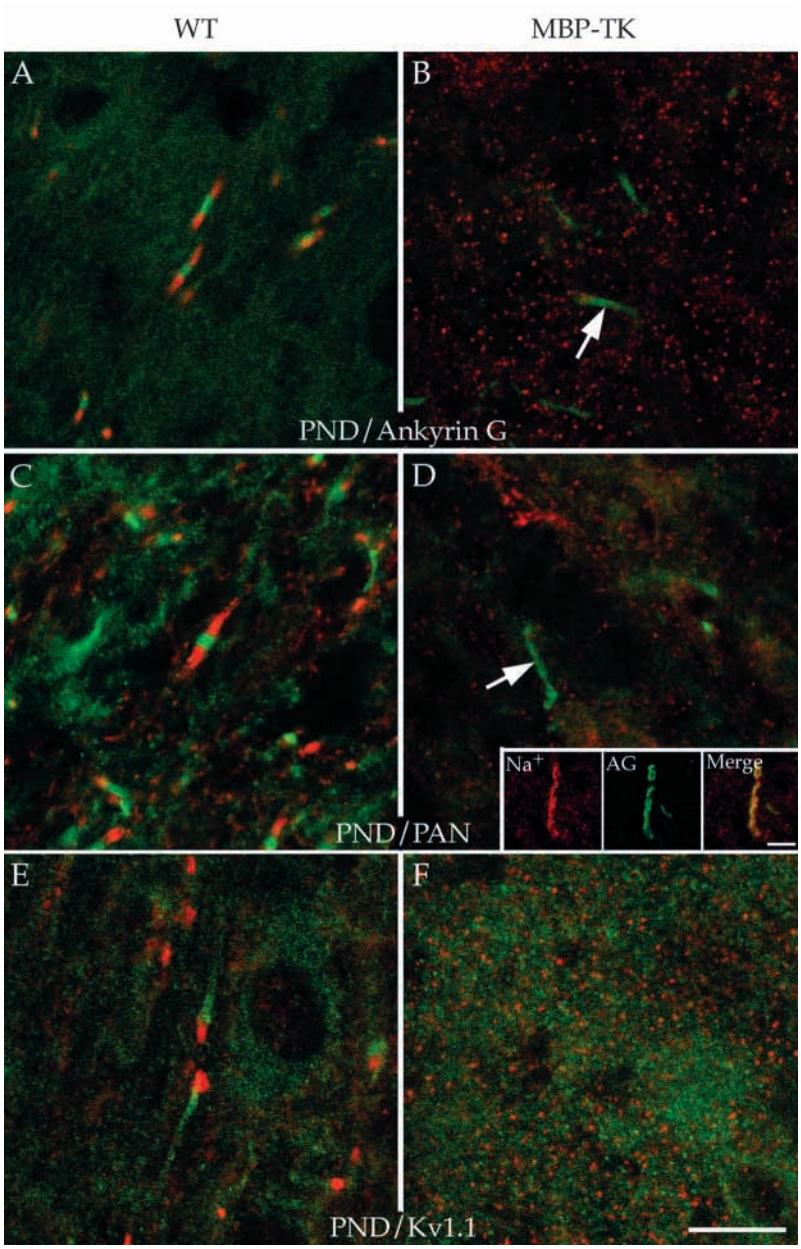

Fig. 1. Distribution of axonal proteins is dramatically altered at nodes of Ranvier in the absence of oligodendrocytes. Brain sections from wild-type (A,C,E) and MBP-TK (B,D,F) animals treated from postnatal day 1 to 20 with FIAU were double-labeled with anti-paranodin (PND) (red) and either anti-ankyrin G (green; A,B), anti-Na$^+$ channel (PAN) (green; C,D) or anti-Kv1.1 (green; E,F) antibodies. Wild-type treated mice show a normal localization of paranodin in the paranodal regions (A,C,E) with typical ankyrin G (A) and Na$^+$ channels clusters (C) distribution in the node of Ranvier. In treated MBP-TK mice, paranodin was not detectable in the paranodes, even if the red was enhanced to reveal nonspecific background (B,D,F). Localization of ankyrin G and Na$^+$ channels was also markedly altered and immunoreactivity was mainly found along the axons (arrows in B,D) of treated MBP-TK animals. Double immunostaining for ankyrin G and Na$^+$ channels showed that these proteins are colocalized (Fig. 1D inset). In contrast to the specific distribution of Kv1.1 clusters in the juxtaparanodes in the wild type (E), K$^+$ channel clustering was completely absent after FIAU treatment in MBP-TK mice (F). Pictures represent single optical sections of the corpus callosum region using confocal scanning microscopy. Scale bars: in F, 10 μm in A-F; in inset, 4 μm.

Surviving oligodendrocytes induce focal paranodin clustering in MBP-TK mice

In 1-20d MBP-TK mice, a few postmitotic pre-existing oligodendrocytes escaped from cell death (5%), as previously

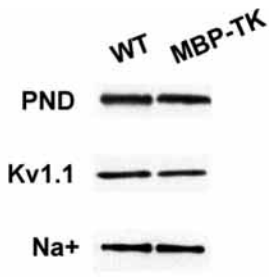

Fig. 2. Protein levels of paranodin, Na^+ and K^+ channel α subunits in the brain of wild-type and MBP-TK mice treated from day 1 to 20. Forebrain tissue from chronically treated (1-20d) wild-type and MBP-TK mice were homogenized as described in the Methods, and equal amounts of proteins were analyzed by immunoblotting (10 μg for paranodin or 30 μg for K^+ and Na^+ channels). No statistical differences in the levels of paranodin (180 kDa), Na^+ channel α subunit (260 kDa) and K^+ channels (86 kDa) were observed after quantification of the western blots (less than 10% variation between samples). The results are representative of three different experiments.

documented (Mathis et al., 2000). We examined whether these surviving oligodendrocytes were still able to direct a focal distribution of paranodal proteins. Double immunostaining of wild-type and MBP-TK brain sections from 1-20d animals was carried out using anti-MBP and anti-paranodin antibodies (Fig. 3). As expected, a very clear reduction of MBP-specific immunostaining was observed in MBP-TK mice. A total absence of myelinated fibers in the cortex and a strong hypomyelination of the corpus callosum was evident in treated transgenic animals (Fig. 3B) in comparison with treated wild-type littermates (Fig. 3A). Anti-paranodin staining showed the presence of numerous paranodes in wild-type mice, always adjacent to MBP labeling along the axon (Fig. 3E).

In the rare myelinated fibers still present in MBP-TK animals, a focal localization of paranodin at the limit of MBP staining was observed (Fig. 3F). However, in most cases the partial myelination of the axon was limited to an isolated segment, and was not sufficient to form binary paranodes. These data strongly support a key role of axon-glial contact in the control of paranodin enrichment at paranodal regions.

Differential alterations of paranodal and nodal regions in 2- and 3-week old *jimpy* mice

Experiments performed in MBP-TK mice allowed us to assess the early involvement of myelinating oligodendrocytes in the organization of membrane domains at the nodes of Ranvier. To investigate a later role of the myelinating cells in the maintenance of these regions, we used the *jimpy* mice. In these mice, a mutation in the proteolipid protein gene (*Plp*) induces aberrant myelin formation and its secondary destruction (Sidman et al., 1964). Myelin deficiency is associated with the abnormal proliferation of oligodendrocytes, and their premature cell death (Knapp et al., 1999; Knapp et al., 1986; Meier and Bischoff, 1974; Vermeesch et al., 1990). The effect of the delayed and spontaneously occurring oligodendrocyte damage on nodal protein distribution, was studied in *jimpy* mice and compared with the results obtained in MBP-TK mice. The localization of nodal and paranodal markers was assessed in the corpus callosum of *jimpy* mice, 2 and 3 weeks after birth (P15 and P21).

In P15 wild-type mice, ankyrin G and Na^+ channels formed typical focal clusters in the nodal regions normally adjacent to paranodes (Fig. 4A, Fig. 5A). Most paranodin immunoreactivity was found in single and binary paranodes (Fig. 4A). At P15, Kv1.1 channel clusters could already be

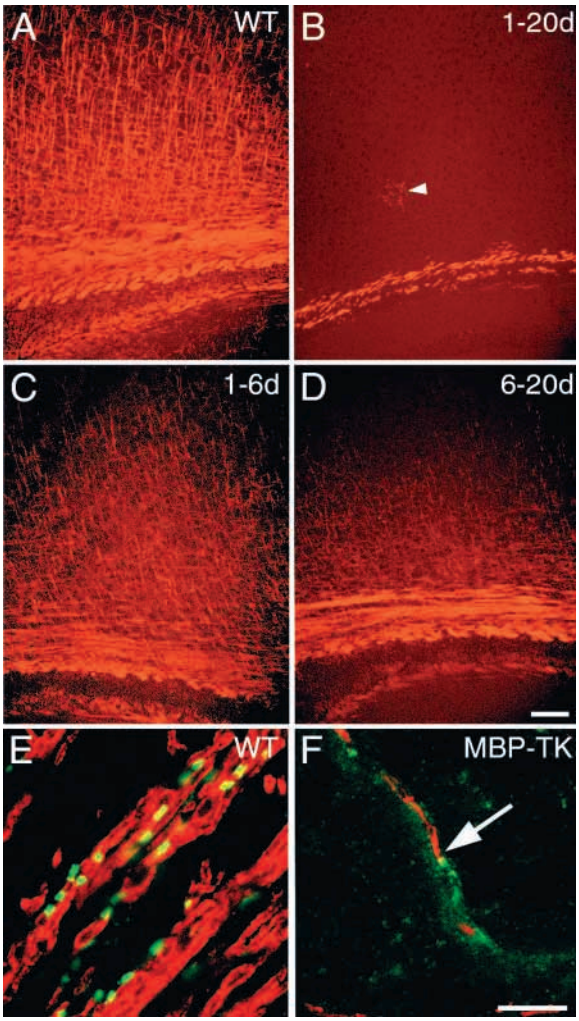

Fig. 3. Immunofluorescence studies of MBP and PND/Caspr in the corpus callosum and the cortex of wild-type and treated MBP-TK mice. Myelinated fibers in the cortex and the corpus callosum are strongly labeled by the MBP antibody in wild-type animals (A). Absence of cortical MBP-positive fibers and a significant reduction of MBP labeling is observed in the corpus callosum of MBP-TK mice (1-20d) (B). Arrowhead in B indicates residual myelinated axons in the first cortical layer of MBP-TK mice brain. MBP-positive myelinated fibers are less abundant in MBP-TK mice corpus callosum after 1-6d treatment (C) than after 6-20d treatment (D). (E,F) Double immunostaining using anti-MBP (red) and anti-paranodin (green) antibodies. The presence of myelin sheaths correlates with the focal localization of paranodin at the paranodal zone in a wild-type animal (E). Paranodin staining is concentrated at the paranode only in myelinated fibers (arrow, F). Scale bars: in D, 100 μm for A-D; in F 10 μm for E,F.

detected in some juxtaparanodal regions (Fig. 5A). At P21, the general pattern of distribution of nodal and paranodal markers in wild-type mice was similar to that described above. A larger proportion of paranodes had a binary aspect at P21 than at P15, and many more K^+ channels-enriched juxtaparanodes were formed (Fig. 5A,C).

The distribution of paranodin and the Kv1.1 potassium channel was dramatically altered in the corpus callosum of *jimpy* mice. At P15, paranodin failed to accumulate at

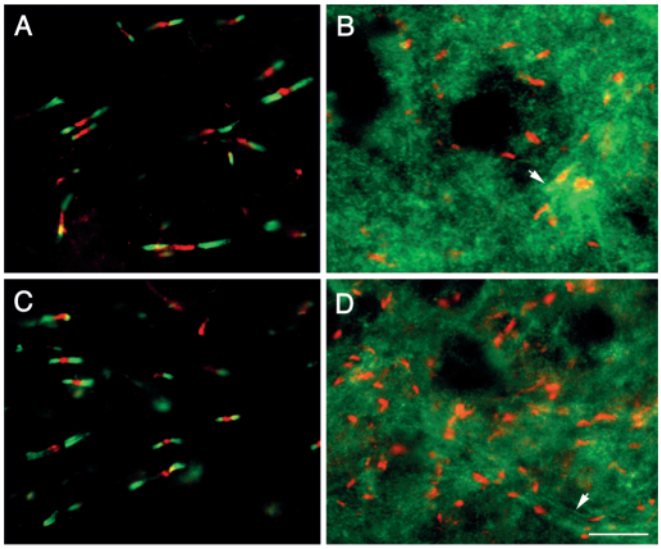

Fig. 4. Localization of ankyrin G and paranodin in *jimpy* mice. Sections from corpus callosum of wild-type (A,C) or *jimpy* (B,D) littermates were examined by double immunostaining with antibodies against paranodin (green) and ankyrin G (red) at postnatal day 15 (A,B) or 21 (C,D). In wild-type mice, paranodin immunoreactivity was concentrated in paranodes, in most instances flanking the nodal aggregates of ankyrin G on either side (A,C). In *jimpy* mice, paranodin immunoreactivity was diffuse, along the axonal membranes (arrows), with no identifiable paranodal cluster. Although ankyrin G clusters were similar in both genotypes at P15, their limits appeared less well delineated in *jimpy* mice at P21. Scale bar: 10 μm.

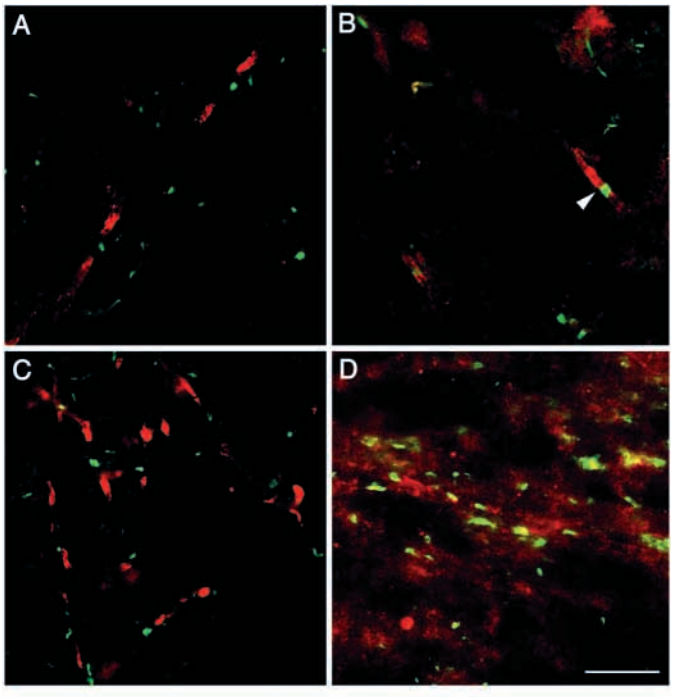

Fig. 5. Localization of Na^+ and K^+ channels in *jimpy* mice. Sections from corpus callosum of wild-type (A,C) or *jimpy* (B,D) littermates were examined by double immunostaining with antibodies against the Na^+ channels (green) and the K^+ channels Kv1.1 (red). Postnatal day 15 (A,B). In wild-type mice, Kv1.1 immunoreactivity was clearly separated from Na^+ channels clusters by an empty space corresponding to paranodes (A). In *jimpy* mice, although the shape of Na^+ and K^+ channel clusters was roughly comparable with that in wild-type littermates, the localization of Kv1.1 immunoreactivity was abnormal as it was not separated from the nodal Na^+ channels (arrowhead, B). Postnatal day 21 (C,D). The alteration of K^+ channels distribution was much more severe than at P15. Immunoreactivity appeared more diffuse, and Kv1.1 aggregates were irregular and fragmented. The shape of Na^+ channels clusters was also altered with fuzzy and irregular limits. Scale bar: 10 μm.

paranodes and was either diffusely distributed or appeared as irregular tiny patches along the axons (Fig. 4B, arrow). At P21, paranodin immunoreactivity remained diffusely distributed along the neuronal membranes (Fig. 4D). Only on rare occasions was accumulation of paranodin detected in the form of single or binary cluster that are characteristic of paranodes (data not shown). Presumably, these infrequent clusters correspond to the few sites of intact myelination that are described in these mice. The localization of K^+ channels was also severely altered in *jimpy* mutants. At P15, in addition to some diffuse immunoreactivity along the axonal processes, Kv1.1 was often found to accumulate at locations that would normally correspond to paranodes, immediately adjacent to the Na^+ channels clusters (Fig. 5B). These abnormal paranodal clusters of K^+ channels tended to disappear at P21 in *jimpy* mice, and most of the immunoreactivity was diffusely distributed along the axons (Fig. 5D). When present, however, the K^+ channel aggregates were in contact, or even overlapped with Na^+ channels clusters (Fig. 5D). Thus, although K^+ channel clustering was observed in *jimpy* mice, it was not localized in juxtaparanodal regions, but was observed close to the nodes. Moreover, the clusters were transient and disappeared 3 weeks after birth.

By contrast, the localization of Na^+ channels and ankyrin G was much less affected in *jimpy* mice than that of paranodin and Kv1.1 channels. At P15, Na^+ channels and ankyrin G were clustered, and outlined nodal segments that appeared similar to those in wild-type controls (Fig. 4B, Fig. 5B). At P21, although most of the Na^+ channel and ankyrin G immunoreactivity remained concentrated in nodal segments, it spread out laterally, displaying an irregular appearance and a blurry outline (Fig. 4D, Fig. 5D). These results indicate that once the nodal clustering of Na^+ channels and ankyrin G has been induced, it persists even in the absence of intact paranodes, at least until the third postnatal week.

Clustering of nodal proteins is independent of paranodin aggregation

The results obtained in 2- and 3-week-old *jimpy* and wild-type mice revealed that nodal clusters were present in the absence of focal paranodin-positive domains. To determine whether a transient aggregation of paranodin might account for the formation of nodal regions in *jimpy* mice, we studied these mice at P8. In the corpus callosum of P8 wild-type mice, focal clusters of Na^+ channels were well defined. Many of these clusters were flanked by single or binary paranodes (Fig. 6A). However, a large proportion of Na^+ channel clusters appeared isolated and were not associated with paranodin immunoreactivity (Fig. 6A). In *jimpy* mice at P8, the overall paranodin staining was more patchy than at later stages (Fig.

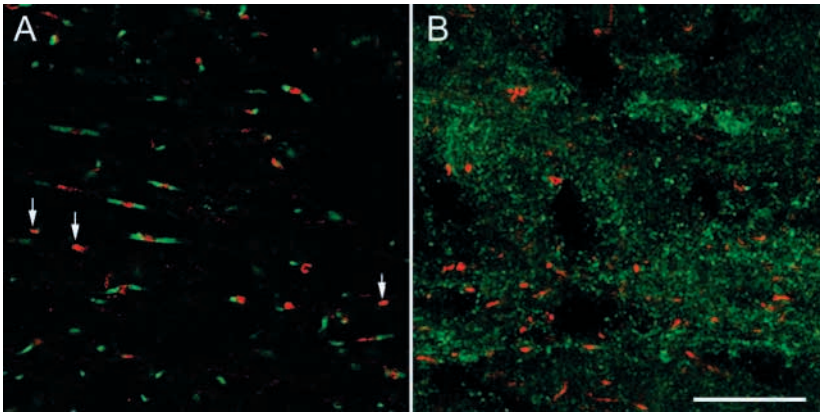

Fig. 6. Early aspect of nodal and paranodal regions in wild-type and *jimpy* mice. Sections from corpus callosum of wild-type (A) or *jimpy* (B) littermates, were examined by double immunostaining with antibodies against paranodin (green) and Na^+ channels (red) at postnatal day 8. In wild-type mice, paranodin immunoreactivity was concentrated in binary or single paranodes, flanking the nodal cluster of Na^+ channels. In many instances, Na^+ channels clusters were observed independently from paranodes (arrows in A). In *jimpy*, paranodin was distributed irregularly, without bona fide identifiable paranodal labeling, whereas the clusters of Na^+ channels appeared essentially normal and comparable with those in wild-type littermates. Scale bar: 20 μm.

6B), an observation that may be related to the targeting of paranodin/contactin complexes to specific membrane domains (Faivre-Sarrailh et al., 2000; Boyle, 2001). However, paranodin immunoreactivity failed to accumulate at paranodes and was irregularly distributed, often forming small aggregates. In spite of the complete disorganization of paranodin localization, Na^+ channels formed nodal clusters that were comparable with those in wild-type controls (Fig. 6). Experiments in which ankyrin G labeling was studied gave results similar to those obtained with Na^+ channels (data not shown). These observations demonstrate that Na^+ channel clusters can form independently of the accumulation of paranodin in paranodes.

Localization of ankyrin G and Na^+ channels in the initial axonal segment is independent of oligodendroglial signaling

Clustering of voltage-gated Na^+ channels is observed not only at the nodes of Ranvier, but also at axon initial segments and at postsynaptic folds of the neuromuscular junction (Catterall, 1981; Wollner and Catterall, 1986). Ankyrin G has been shown to direct Na^+-channel cluster localization to the initial segments of Purkinje cell axons (Zhou et al., 1998). Because in vivo ablation of oligodendrocytes strongly perturbed the nodal distribution of ankyrin G and voltage-gated Na^+ channels, the localization of these proteins was also analyzed in the initial segments of cortical pyramidal axons in treated MBP-TK mice. Axons from these neurons were well myelinated in wild-type animals (Fig. 3A), while a complete absence of MBP staining was observed in the cortex of transgenic treated mice (Fig. 3B). No difference in the localization of ankyrin G and Na^+ channels in the initial axonal segment of cortical neurons was observed between treated wild-type and transgenic mice (Fig. 7). These results clearly show that the formation of clusters in the initial axon segments is independent of oligodendroglial signals. Thus, two different molecular mechanisms appear to be responsible for organizing the distribution of ankyrin G and Na^+ channels in the axonal initial segment and in the node of Ranvier.

DISCUSSION

The presence of oligodendrocytes is crucial for the organization of axonal paranodal domains

Paranodal junctions are one of the sites of attachment of oligodendrocytes to axons. Paranodin/Caspr is an axonal glycoprotein highly enriched in these specialized junctions (Einheber et al., 1997; Menegoz et al., 1997). Although the mechanisms responsible for the localization of paranodin to axon-glial junctions are not yet fully established, results in several dysmyelinating mutants reveal that contacts with myelinating oligodendrocytes are essential. Paranodal enrichment of paranodin is lost in *Cgt*$^{-/-}$ mice, which are deficient in galactocerebrosides and sulfatides, and present abnormal paranodal junctions (Dupree et al., 1999). Ablation of oligodendrocytes in MBP-TK mice completely abolishes the normal localization of paranodin. This alteration seems to be dependent on the degree of dysmyelination, as it correlates with the extent of oligodendrocyte loss observed after different FIAU treatments. Furthermore, the rare myelinating oligodendrocytes in the MBP-TK mice brains were associated with localized focal enrichment of paranodin close to MBP-positive domains. This strongly points to an absolute requirement of myelinating oligodendrocytes for the organization of the paranodal axolemma. This is also supported by the dramatic alteration of paranodin distribution observed in *jimpy* mice, at all ages examined.

Oligodendrocytes influence the localization, but not the expression of paranodin, as its protein level is unaltered in MBP-TK treated mice (Fig. 2), as well as in *jimpy* mice (N. D.

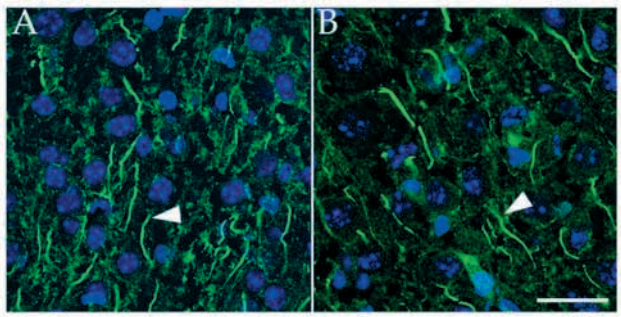

Fig. 7. Localization of Na^+ channel clusters in the initial axonal segment of cortical neurons. Comparable brain sections from wild-type (A) and treated MBP-TK (B) 1-20d mice were immunolabeled with anti-Na^+ channel (PAN) antibodies. Nuclei of cortical neurons are visualized with DAPI staining. In both wild-type and treated MBP-TK animals, we observed a high concentration of Na^+ channels (A,B) in the initial axonal segment of the cortical pyramidal neurons (arrowheads). Scale bar: 30 μm.

and J. A. G., unpublished), and *Cgt*$^{-/-}$ mice (Dupree et al., 1999). Furthermore, diffuse paranodin immunoreactivity was detected along axons in both types of mutants. Thus, proper localization of paranodin is likely to result from its interaction with oligodendroglial partner(s). The 155 kDa isoform of neurofascin (NF155), which is selectively enriched in oligodendrocytes paranodal loops, is a candidate for participating in such complexes (Tait et al., 2000). However, NF155 does not appear to associate directly with paranodin (Tait et al., 2000). However, paranodin/Caspr is associated with contactin in the axonal membrane (Rios et al., 2000), and this association is crucial for its expression at the cell surface (Faivre-Sarrailh et al., 2000; Boyle et al., 2001). Thus, interactions of paranodin with glial partners, might be mediated through contactin or through other unidentified proteins.

The role of oligodendrocytes in the formation and maintenance of K^+ channel clusters and their segregation from nodal regions

One of the proposed roles of the paranodal septate-like junctions is to demarcate axonal domains by limiting the lateral diffusion of axonal proteins. During myelination, Shaker-type K^+ channels appear in the juxtaparanodal zone following paranode formation and nodal clustering of Na^+ channels (Rasband and Shrager, 2000). Exclusion of K^+ channels from axoglial junctions and formation of compact myelin are both required for initiation and maintenance of K^+ clusters (Baba et al., 1999; Dupree et al., 1999; Rasband et al., 1999b). The results in MBP-TK mice also underlined the essential role of oligodendrocytes in K^+ channel clustering. In 1-20d FIAU-treated MBP-TK mice, despite the unaltered levels of Kv1.1, the distribution in axonal membranes was completely diffuse. No juxtaparanodal Kv1.1-positive domains were identified in transgenic mice despite the presence of a few paranodes. Similarly, in 1-6d and 6-20d mice, the localization of K^+ channels was more severely disrupted than that of other markers of Ranvier nodes.

The study of *jimpy* mice provided additional information on the organization of axonal Kv1.1 clusters. In 2-week-old *jimpy* mice, although some K^+ channel clusters were formed, they were directly adjacent to nodal regions, as though they were repelled from the internodes and/or attracted to the nodes. Similar observations have been reported in *Cgt*$^{-/-}$ mice, contactin and NCP1 deficient mice (Bhat et al., 2001; Boyle et al., 2001; Dupree et al., 1999). This is clearly different from the fate of paranodin, which was diffusely distributed in the two types of mutant mice. The mechanism(s) responsible for the K^+ channel 'juxta-nodal' positioning is not known and may involve their association with other neuronal proteins, including Caspr2, and, possibly, extracellular partners when paranodes are absent. These results also show that K^+-channel clustering is supported by a mechanism independent of paranodin accumulation in axoglial junctions. The paranodal septate-like junctions, and possibly paranodin itself, are crucial for the separation of K^+ channels from the nodal region. In addition, oligodendrocytes are necessary for the maintenance of K^+-channel clusters as Kv1.1 immunoreactivity was diffused in 3-week-old *jimpy* mice or appeared as irregular and fragmented aggregates. This progressive alteration of K^+ channel distribution paralleled the extent of myelin degeneration.

The role of oligodendrocytes in the initial organization of the nodal regions

An important aspect of our results is related to the organization of nodal regions. Ankyrin G is a membrane-associated spectrin-binding protein, which interacts directly with voltage-gated Na^+ channels in the axoplasm (Lambert et al., 1997; Srinivasan et al., 1988; Zhou et al., 1998). It has been suggested that neuronal ankyrin G plays a role in the targeting, clustering and stabilization of Na^+ channels (Zhou et al., 1998). In nodal regions, ankyrin G interacts also with the cell adhesion molecules NF155 and NrCAM, which may be involved in the formation of nodal clusters (Trapp and Kidd, 2000). Our results in treated MBP-TK mice demonstrate that in the absence of oligodendrocytes, Na^+ channels are normally expressed but fail to accumulate in nodal regions. Indeed, the analysis of 1-20d FIAU-treated mice showed the presence of only few broad nodes where Na^+ channels and ankyrin G colocalize. These figures were also observed in wild-type animals, although to a much lower extent, and might represent an early stage of nodal formation.

Despite the loss of nodal clustering of ankyrin G and Na^+ channels in MBP-TK mice, a normal accumulation of these proteins was observed in the initial segment of cortical axons. This demonstrates that ankyrin G and Na^+-channel clustering in this location is functional in the absence of oligodendrocytes.

The molecular mechanism responsible for Na^+-channel sequestration at the nodes of Ranvier in CNS axons is not known. In vitro, Na^+ channel/ankyrin G clustering seems dependent upon a diffusible, unidentified factor, that is produced by oligodendrocytes (Kaplan et al., 1997). Conversely, paranodal axoglial contacts were proposed to be a pre-requisite for this nodal clustering in vivo (Rasband et al., 1999a). However, the results in dysmyelinating mutants, were not fully conclusive. Indeed, although the number of nodal aggregates is decreased in myelin-deficient rats (Kaplan et al., 1997) and in *shiverer* mice (Rasband et al., 1999a), several nodes appear to be normally formed. Moreover, nodal regions are relatively spared in galactolipid-deficient mice, as well as in contactin and paranodin mutants, in spite of severe alterations of the paranodal regions (Dupree et al., 1999; Boyle, 2001; Bhat, 2001). Experiments using MBP-TK mice convincingly demonstrate that oligodendrocytes are necessary for the clustering of nodal proteins, and suggest that, if a diffusible factor is involved, its range of action is very limited.

The results in wild-type and *jimpy* mice provide additional insights into the formation and maintenance of nodal regions. In the corpus callosum of 1-week-old wild-type mice, many nodal clusters of Na^+ channels (Fig. 6) and of ankyrin G (data not shown) were observed independently of paranodin aggregates. This indicates that nodal clusters form before and independently of the accumulation of paranodin in axoglial junctions, in contrast to previous reports in the optic nerve (Rasband et al., 1999a). Interestingly, comparable results have been reported in the peripheral nervous system (Melendez-Vasquez et al., 2001). Similarly, nodal clusters were identifiable in *jimpy* mice at P8, P15 and even P21, despite a complete disappearance of paranodin clusters. However, in 3-

week-old *jimpy* mice, nodal clusters started to deteriorate, losing their well-defined limits. Altogether these results show that oligodendrocytes are necessary at an early stage of myelination for the accumulation of Na^+ channels and ankyrin G at the nodes of Ranvier. This effect involves early, short-range interactions between oligodendrocytes and axons, but does not require the accumulation of paranodin in axoglial contacts. However, lack of paranodal junctions results in unstable nodal regions, which progressively become less well defined.

Conclusion

Our results, together with those of others (Peles and Salzer, 2000; Rasband and Shrager, 2000), delineate the role of oligodendrocytes in the organization of membrane domains in myelinated axons of CNS neurons. The organization of neuronal proteins, including paranodin, ankyrin G, Na^+ and K^+ channels, along the axon is controlled by oligodendrocytes, whereas their expression is independent. In the absence of oligodendrocytes, nodal, paranodal and juxtaparanodal regions are no longer identifiable. Aggregation of paranodin appears to be particularly sensitive to alterations of oligodendrocytes. The tight dependence of paranodin clustering on oligodendrocytes is not surprising as this protein is part of the paranodal adhesion complexes that form between axons and oligodendrocytes. By contrast, once they are formed, K^+ and Na^+ channel clusters appear to be more resistant than paranodal regions to lesions of oligodendrocytes. These ion channels are not part of intercellular junctions, and their aggregation might be mostly dependent on their association with cytoskeletal proteins in the axoplasm and in the axolemma (e.g. ankyrin G for Na^+ channels and Caspr2 for K^+ channels). However, when paranodes are absent or altered, the limits of clusters comprising either Na^+ channels/ankyrin G or K^+ channels become less defined and the normal separation between nodal and juxtaparanodal domains disappears. This indicates that paranodes prevent lateral diffusion of proteins of the axolemma.

We acknowledge Brystol Myers Squibb for generously providing FIAU. We are grateful to J. L. Vonesch, D. Hentsch and M. Boeglin for confocal image analyses. A special thanks to V. Heidt and E. Erbs for help and support and S. Tan for discussions. C. M. was supported by fellowships from the French Ministère de l'Education Nationale, de la Recherche et de la Technologie, and the Association pour la Recherche sur le Cancer. We thank Dr B. Zalc and Prof. C. Lubetzki (INSERM U495) for providing *jimpy* mice, and Dr R. Levinson for providing the rabbit antibodies against Na^+ channels. Pascal Ezan is gratefully acknowledged for his help with immunohistofluorescence. This work has been funded by grants from INSERM, CNRS, CHU and Aventis to E. B.

REFERENCES

Baba, H., Akita, H., Ishibashi, T., Inoue, Y., Nakahira, K. and Ikenaka, K. (1999). Completion of myelin compaction, but not the attachment of oligodendroglial processes triggers K^+ channel clustering. *J. Neurosci. Res.* **58**, 752-764.

Bhat, M. A., Rios, J. C., Lu, Y., Garcia-Fresco, G. P., Ching, W., St Martin, M., Li, J., Einheber, S., Chesler, M., Rosenbluth, J. et al. (2001). Axon-glia interactions and the domain organization of myelinated axons requires Neurexin IV/Caspr/Paranodin. *Neuron* **30**, 369-383.

Borrelli, E., Heyman, R., Hsi, M. and Evans, R. M. (1988). Targeting of an inducible toxic phenotype in animal cells. *Proc. Natl. Acad. Sci. USA* **85**, 7572-7576.

Boyle, M. E. T., Berglund, E. O., Murai, K. K., Weber, L., Peles, E. and Ranscht, B. (2001). Contactin orchestrates assembly of the septate-like junctions at the paranode in myelinated peripheral nerve. *Neuron* **30**, 385-397.

Catterall, W. A. (1981). Localization of sodium channels in cultured neural cells. *J. Neurosci.* **1**, 777-783.

Dupree, J. L., Girault, J. A. and Popko, B. (1999). Axo-glial interactions regulate the localization of axonal paranodal proteins. *J. Cell Biol.* **147**, 1145-1152.

Einheber, S., Zanazzi, G., Ching, W., Scherer, S., Milner, T. A., Peles, E. and Salzer, J. L. (1997). The axonal membrane protein Caspr, a homologue of neurexin IV, is a component of the septate-like paranodal junctions that assemble during myelination. *J. Cell Biol.* **139**, 1495-1506.

Faivre-Sarrailh, C., Gauthier, F., Denisenko-Nehrbass, N., Le Bivic, A., Rougon, G. and Girault, J.-A. (2000). The glycosylphosphatidyl Inositol-anchored adhesion molecule F3/Contactin is required for surface transport of Paranodin/Contactin-associated protein (caspr). *J. Cell Biol.* **149**, 491-501.

Kaplan, M. R., Meyer-Franke, A., Lambert, S., Bennett, V., Duncan, I. D., Levinson, S. R. and Barres, B. A. (1997). Induction of sodium channel clustering by oligodendrocytes. *Nature* **386**, 724-728.

Knapp, P. E., Bartlett, W. P., Williams, L. A., Yamada, M., Ikenaka, K. and Skoff, R. P. (1999). Programmed cell death without DNA fragmentation in the *jimpy* mouse: secreted factors can enhance survival. *Cell Death Differ.* **6**, 136-145.

Knapp, P. E., Skoff, R. P. and Redstone, D. W. (1986). Oligodendroglial cell death in *jimpy* mice: an explanation for the myelin deficit. *J. Neurosci.* **6**, 2813-2822.

Lambert, S., Davis, J. Q. and Bennett, V. (1997). Morphogenesis of the node of Ranvier: co-clusters of ankyrin and ankyrin-binding integral proteins define early developmental intermediates. *J. Neurosci.* **17**, 7025-7036.

Mathis, C., Hindelang, C., LeMeur, M. and Borrelli, E. (2000). A transgenic mouse model for inducible and reversible dysmyelination. *J. Neurosci.* **20**, 7698-7705.

Meier, C. and Bischoff, A. (1974). Dysmyelination in '*jimpy*' mouse. Electron microscopic study. *J. Neuropathol. Exp. Neurol.* **33**, 343-353.

Melendez-Vasquez, C. V., Rios, J. C., Zanazzi, G., Lambert, S., Bretscher, A. and Salzer, J. L. (2001). Nodes of Ranvier form in association with ezrin-radixin-moesin (ERM)-positive Schwann cell processes. *Proc. Natl. Acad. Sci. USA* **98**, 1235-1240.

Menegoz, M., Gaspar, P., Le Bert, M., Galvez, T., Burgaya, F., Palfrey, C., Ezan, P., Arnos, F. and Girault, J. A. (1997). Paranodin, a glycoprotein of neuronal paranodal membranes. *Neuron* **19**, 319-331.

Moll, C., Mourre, C., Lazdunski, M. and Ulrich, J. (1991). Increase of sodium channels in demyelinated lesions of multiple sclerosis. *Brain Res.* **556**, 311-316.

Noebels, J. L., Marcom, P. K. and Jalilian-Tehrani, M. H. (1991). Sodium channel density in hypomyelinated brain increased by myelin basic protein gene deletion. *Nature* **352**, 431-434.

Peles, E. and Salzer, J. L. (2000). Molecular domains of myelinated axons. *Curr. Opin. Neurobiol.* **10**, 558-565.

Poliak, S., Gollan, L., Martinez, R., Custer, A., Einheber, S., Salzer, J. L., Trimmer, J. S., Shrager, P. and Peles, E. (1999). Caspr2, a new member of the neurexin superfamily, is localized at the juxtaparanodes of myelinated axons and associates with K^+ channels. *Neuron* **24**, 1037-1047.

Rasband, M. N. and Shrager, P. (2000). Ion channel sequestration in central nervous system axons. *J. Physiol.* **525**, 63-73.

Rasband, M. N., Peles, E., Trimmer, J. S., Levinson, S. R., Lux, S. E. and Shrager, P. (1999a). Dependence of nodal sodium channel clustering on paranodal axoglial contact in the developing CNS. *J. Neurosci.* **19**, 7516-7528.

Rasband, M. N., Trimmer, J. S., Peles, E., Levinson, S. R. and Shrager, P. (1999b). K^+ channel distribution and clustering in developing and hypomyelinated axons of the optic nerve. *J. Neurocytol.* **28**, 319-331.

Rios, J. C., Melendez-Vasquez, C. V., Einheber, S., Lustig, M., Grumer, M., Hemperly, J., Peles, E. and Salzer, J. L. (2000). Contactin-associated protein (Caspr) and contactin form a complex that is targeted to the paranodal junctions during myelination. *J. Neurosci.* **20**, 8354-8364.

Salzer, J. L. (1997). Clustering sodium channels at the node of Ranvier: Close encounters of the axon-glia kind. *Neuron* **18**, 843-846.

Sidman, R. L., Dickie, M. M. and Appel, S. H. (1964). Mutant mice (*quaking* and *Jimpy*) with deficient myelination in the central nervous system. *Science* **144**, 309-311.

Srinivasan, Y., Elmer, L., Davis, J., Bennett, V. and Angelides, K. (1988). Ankyrin and spectrin associate with voltage-dependent sodium channels in brain. *Nature* **333**, 177-180.

Tait, S., Gunn-Moore, F., Collinson, J. M., Huang, J., Lubetzki, C., Pedraza, L., Sherman, D. L., Colman, D. R. and Brophy, P. J. (2000). An oligodendrocyte cell adhesion molecule at the site of assembly of the paranodal axo-glial junction. *J. Cell Biol.* **150**, 657-666.

Trapp, B. D. and Kidd, G. J. (2000). Axo-glial septate junctions. The maestro of nodal formation and myelination? *J. Cell Biol.* **150**, F97-F100.

Vermeesch, M. K., Knapp, P. E., Skoff, R. P., Studzinski, D. M. and Benjamins, J. A. (1990). Death of individual oligodendrocytes in *jimpy* brain precedes expression of proteolipid protein. *Dev. Neurosci.* **12**, 303-315.

Wang, H., Allen, M. L., Grigg, J. J., Noebels, J. L. and Tempel, B. L. (1995). Hypomyelination alters K^+ channel expression in mouse mutants *shiverer* and *Trembler*. *Neuron* **15**, 1337-1347.

Wang, H., Kunkel, D. D., Martin, T. M., Schwartzkroin, P. A. and Tempel, B. L. (1993). Heteromultimeric K+ channels in terminal and juxtaparanodal regions of neurons. *Nature* **365**, 75-79.

Westenbroek, R. E., Noebels, J. L. and Catterall, W. A. (1992). Elevated expression of type II Na^+ channels in hypomyelinated axons of shiverer mouse brain. *J. Neurosci.* **12**, 2259-2267.

Wollner, D. A. and Catterall, W. A. (1986). Localization of sodium channels in axon hillocks and initial segments of retinal ganglion cells. *Proc. Natl. Acad. Sci. USA* **83**, 8424-8428.

Zhou, D., Lambert, S., Malen, P. L., Carpenter, S., Boland, L. M. and Bennett, V. (1998). AnkyrinG is required for clustering of voltage-gated Na^+ channels at axon initial segments and for normal action potential firing. *J. Cell Biol.* **143**, 1295-1304.